ELSEVIER

Journal of Chromatography A, 887 (2000) 265–275

JOURNAL OF CHROMATOGRAPHY A

www.elsevier.com/locate/chroma

Capillary electrochromatography using continuous-bed columns of sol–gel bonded silica particles with mixed-mode octadecyl and propylsulfonic acid functional groups

Qinglin Tang, Milton L. Lee*

Department of Chemistry and Biochemistry, Brigham Young University, Provo, UT 84602-5700, USA

Abstract

Continuous-bed columns containing sol–gel bonded 3 μm silica particles with mixed-mode octadecyl and propylsulfonic acid functional groups (ODS/SCX) were prepared by first packing the ODS/SCX particles into a fused-silica capillary, then filling the packed capillary with a siliceous sol–gel, curing the sol–gel, and finally drying the column with supercritical carbon dioxide. The performance of the sol–gel bonded ODS/SCX columns was evaluated for capillary electrochromatography using acetonitrile aqueous mobile phase containing phosphate buffer. The columns were mechanically strong and permeable. Both EOF velocity and current increased linearly with elevation of the applied electric field strength. The EOF velocity was high at low pH and nearly constant over a range of pH 2–9. Higher buffer concentration resulted in higher current and lower EOF velocity. The acetonitrile content had no significant effect on the EOF. Without thermosetting the column, no bubble formation was noticed with currents up to 2.5 μA. The minimum plate height of a 25/34 cm×75 μm I.D. sol–gel bonded 3 μm ODS/SCX column was 5.7 μm (1.75×10^5 plates per meter) at an optimum EOF velocity of 0.92 mm s^{-1}. Mixtures of test aromatic compounds and aromatic hydrocarbon homologues gave symmetrical peaks when using a low pH mobile phase. The retention and elution order of aromatic compounds represented a typical reversed-phase separation mechanism similar to conventional ODS columns. The run-to-run and column-to-column retention factor reproducibility was better than 2.5% and 8.0% RSD, respectively.

Keywords: Sol–gel; Stationary phases, CEC; Electrochromatography

1. Introduction

Capillary electrochromatography (CEC), a hybrid of capillary electrophoresis and high-performance liquid chromatography (LC), continues to develop into a potentially useful liquid phase microseparation technique [1–10]. In CEC, the mobile phase moves through a capillary column (typically 50–100 μm I.D.) by electroosmotic flow (EOF) generated in the column under an applied electric field across the length of the column. High efficiency in terms of plates per meter can be obtained in CEC since the EOF is plug-like, and high efficiency in terms of plates per column can also be achieved by the use of small particles and long columns due to the absence of column back pressure. In addition, CEC consumes small sample volumes and is easy to interface with mass spectrometry due to the use of miniaturized columns. Furthermore, CEC combines the separation mechanisms of LC and CE, and compounds can be separated according to their partition coefficients, electrophoretic mobilities, or a combination of both.

CEC is still a relatively new technique, and much

*Corresponding author. Tel.: +1-801-378-2135; fax: +1-801-378-5474.

0021-9673/00/$ – see front matter
PII: S0021-9673(99)01196-6

research must be done to realize its full potential. One of the most urgent needs is improved column technology. A CEC column requires functional groups for selectivity and charged groups for EOF. Most of the columns reported for CEC are capillaries packed with octadecylsilica (ODS) particles of 1.5–5 μm diameter. The residual silanols on the surface of the silica support serve as EOF generating groups, and the octadecyl chains function as separating groups. Two major problems have been associated with the use of typical packed capillary ODS columns in CEC. First, it is difficult to fabricate integrated end-frits with the same properties of the packing materials [11,12]. Poorly prepared end-frits often cause bubble formation and peak tailing and, thus, pressurization of the column is required, which complicates the CEC instrumentation and operation. Second, dissociation of silanol groups on the surface of the silica support is pH dependent, leading to a very small EOF at low pH and an increased EOF as pH increases [13]. The EOF dependency on pH can cause irreproducible retention times, and the small EOF at low pH limits the separation speed and useful pH operating range.

To circumvent the challenges posed by the use of end-frits, open-tubular columns have been used for CEC [14–16]. However, the small sample capacity of open-tubular columns limits their use to samples with low concentration dynamic ranges.

Recently, continuous-bed, sometimes called monolithic, columns have shown great potential for CEC because they have high sample capacity and no end-frits [17–32]. Several types of continuous-bed columns including organic polymer [17–23], silica-based sol–gel [24–26], and particle-fixed [27–32] columns have been developed for CEC. The control of pore size and rigidity are key to the success of organic polymer continuous-bed columns. Care must also be paid to prevent drying of the organic polymer continuous bed. Silica-based sol–gel continuous-bed columns suffer from shrinking and/or cracking of the column bed, which results in low efficiency or even total column failure.

Particle-fixed continuous-bed columns are designed to inherit the selectivities of packing materials used in LC. Dulay et al. [27] prepared an ODS particle-loaded continuous-bed column using a silicate sol–gel as loading matrix. The ODS-loaded continuous-bed column demonstrated high permeability and alleviated column bed cracking. However, only a moderate efficiency of 80,000 plates per meter for a 3 μm ODS-loaded column was obtained, which was believed to resulted from the inhomogeneous ODS loading in the matrix. Asiaie et al. [28] and Adam et al. [29] fabricated an ODS particle-fused continuous-bed column using a sintering process. An efficiency of 125 000 plates per meter for a 6 μm ODS column was achieved. However, the experimental conditions used in the sintering process were so harsh that the stationary phase was destroyed and post deactivation and functionalization of the sintered bed were necessary. Chirica et al. [30] reported particle-entrapped continuous-bed columns using a silicate sol–gel as an entrapping matrix. An efficiency of 12 000 plates per meter was demonstrated. However, it took several days to dry the column, and the column induced peak tailing. In previous papers, we reported sol–gel bonded ODS continuous-bed columns using an inert sol–gel derived from tetramethoxysilane and ethyltrimethoxysilane as a bonding agent and supercritical CO_2 as a column drying agent [31,32]. The fabrication of these sol–gel bonded monolithic columns was easy, and required a relatively short preparation time. The resultant columns were inert, efficient, and selective.

In an effort to manipulate the EOF, packed columns containing silica-based packing materials with mixed-mode functional groups (i.e., long hydrocarbon chains and sulfonic acid) for CEC have been reported [33–36]. Strong EOF at low pH and relatively stable EOF throughout a wide pH range were found with these columns.

In this study, we extended our sol–gel continuous-bed column technology to the preparation of sol–gel bonded columns containing silica particles with mixed-mode octadecyl and propylsulfonic acid functional groups (ODS/SCX). The characteristics of these sol–gel bonded ODS/SCX continuous-bed columns for CEC are discussed.

2. Experimental

2.1. Materials and chemicals

Fused silica capillaries of 75 μm I.D. and 360 μm O.D. were purchased from Polymicro Technologies (Phoenix, AZ, USA). A Lee Scientific Model 600

SFC pump (Dionex, Salt Lake Division, Salt Lake City, UT, USA) was used to pack the capillaries and to dry the sol–gel bonded column. A 250 μl PEEK™ syringe (Unimetrics, Shorewood, IL, USA) mounted on a syringe driver (PHD2000, Harvard Apparatus, Holliston, MA, USA) was used to fill the columns with sol solution. A Phoenix 20 LC pump (Fisons Instruments, Milan, Italy) was used to rinse the columns with acetonitrile. An experimental batch of Spherisorb S3 ODS/SCX particles with mixed-mode octadecyl and propylsulfonic acid (3 μm, 80 Å) was provided by Peter Myers of Xtec (Stockport, Cheshire, UK).

Tetramethoxysilane (TMOS) and ethyltrimethoxysilane (ETMOS) were purchased from Gelest (Tullytown, PA, USA). Other chemicals were obtained from Sigma (St. Louis, MO, USA) and Aldrich (Milwaukee, WI, USA). HPLC grade water was purchased from Mallinckrodt Chemicals (Paris, KY, USA). Aqueous trifluoroacetic acid (TFA) solution at pH 2 was prepared by adding TFA into water until a pH of 2 was reached as measured with short-range Alkacid pH test paper (Micro Essential Laboratory, NY, USA)

A phosphate buffer stock solution was prepared by mixing appropriate volumes of 50 m*M* sodium monophosphate and 50 m*M* phosphoric acid to give the desired pH. The mobile phase was prepared by diluting the stock buffer solution with appropriate volumes of water and acetonitrile to obtain the desired buffer concentration and pH. The mobile phase was filtered through a 0.45 μm pore nitrocellulose filter (Micron Separations, Westborough, MA, USA) and sonicated for 10 min to chase out any dissolved air bubbles before use. Test mixtures of aromatic compounds (0.3 m*M* thiourea, 11.6 m*M* benzylalcohol, 1.7 m*M* benzaldehyde, 0.3 m*M* dimethylphthalate, 0.2 m*M* benzophenone, and 0.3 m*M* biphenyl), and aromatic hydrocarbon homologues (0.03 m*M* benzene, 0.03 m*M* toluene, 0.03 m*M* ethylbenzene, and 0.03 m*M* butylbenzene) were prepared by first dissolving an appropriate amount of each pure chemical into acetonitrile and then diluting with a solution of the same composition as the mobile phase.

2.2. Preparation of continuous-bed columns

The preparation of continuous-bed columns was similar to that described in our previous paper [31]. In short, a length of fused-silica capillary was washed with 1 *M* KOH, followed by water, and dried with nitrogen at 120°C. The capillary was packed using a carbon dioxide slurry method [37] with pressure increasing from 5 to 25 MPa at a rate of 0.5 MPa per min in a sonicator bath. An 8% sol solution with a composition of 18 μl TMOS, 18 μl ETMOS, 12 μl aqueous TFA solution at pH 2, 200 μl methanol, and 200 μl formamide was pushed into the packed capillary until the sol solution reached a position of 12 cm from the column outlet observed with the naked eye. Then both ends of the column were sealed using two silicone septa, and the column was left alone for gelling and curing at room temperature for 24 h. The cured column was flushed with supercritical CO_2 at 8 MPa and 40°C to replace the solvent and then dried by temperature programming from 40°C to 250°C at a rate of 1°C per min and maintaining the temperature at 250°C for 1 h. The particles at the end of the column that were not bonded by the sol–gel were flushed out and a UV detection window was prepared immediately after the column bed by dissolving away the polyimide coating with concentrated ammonium hydroxide. In several cases, a short length of the column was cut off and sputtered with a gold coating of approximately 100 Å thick for observation of the cross-section of the column bed with a scanning electron microscope (JEOL JSN 840A).

2.3. CEC experiments

CEC experiments were carried out using a homemade capillary electrochromatograph without pressurization of the column as described in a previous paper [31]. Before installing it in the CEC instrument, the column was thoroughly rinsed with degassed 80% acetonitrile aqueous solution containing 1.5 m*M* pH 7 phosphate buffer under 5 MPa pressure with the inlet end of the column connected to a Phoenix 20 pump and the outlet end inserted into the outlet vial through the on-column UV detection flow cell. A voltage of 5 kV was then applied across the length of the column until a stable current was obtained, which usually required less than 1 h. Finally the column was conditioned for 30 min at 30 kV applied voltage. Samples dissolved in a solution

of the mobile phase were introduced into the column by electrokinetic injection. Thiourea (0.3 m*M*) was used as an EOF marker.

3. Results and discussion

3.1. Preparation of continuous-bed columns

Scanning electron micrographs of the ends of sol–gel bonded continuous bed columns containing 3 μm ODS/SCX particles showed that the particles were bonded to each other and to the inner walls of the capillaries through a sol–gel matrix, forming a continuous bed. Fig. 1 shows the synthetic scheme for preparation of the sol–gel and sol–gel bonded ODS/SCX particles. Under acidic conditions, TMOS and ETMOS undergo hydrolysis and polycondensation, forming a sol–gel. Because TMOS has a higher polycondensation rate than ETMOS in acidic solution [38], TMOS forms a silica backbone and ETMOS forms an outer coating. The sol–gel matrix is, thus, a silica network endcapped with an inert layer of ethyl groups. Different from the silica matrix used in particle-entrapped [30] and particle-loaded [27] continuous-bed columns, the sol–gel matrix in our sol–gel bonded columns was inert. The sol–gel matrix formed chemical bonds to the surface of the particles and to the walls through polycondensation of the silanols in the sol–gel matrix, on the column walls and on the ODS/SCX particles. Because the sol–gel matrix is open, mobile phases and solutes can still access the octadecyl and propylsulfonic acid functional groups.

In our previous work [31,32], we found that the percentages of precursors in the sol solution were important for a good sol–gel bonded continuous-bed column. In the preparation of the sol–gel bonded ODS/SCX columns, different percentages of precursors in the sol solution were evaluated. It was observed that the permeability and mechanical strength of the column was dependent on the percentage of sol–gel precursors. A high percentage of sol–gel precursors resulted in low permeability, but high mechanical strength. While the concentrations of the precursors in the sol solution were not optimized for the ODS/SCX columns, a column containing 8% sol–gel bonded particles showed good mechanic strength and permeability. No change in the column bed was observed after the column was rinsed for 24 h and used in CEC for 3 weeks.

No cracking or shrinking of the column bed was observed for the sol–gel bonded ODS/SCX column. This is an advantage of this column over the pure sol–gel column [26]. In pure sol–gel columns, reduction in volume due to polycondensation and

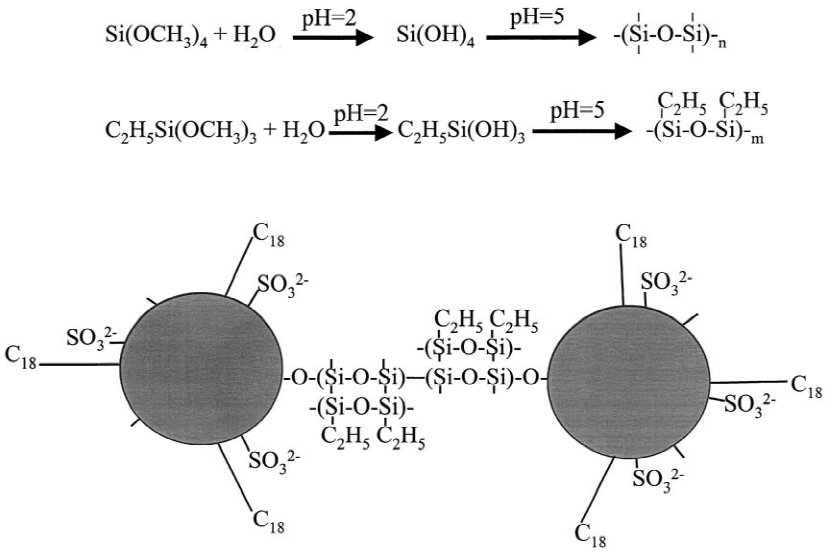

Fig. 1. Synthetic scheme for the sol–gel and sol–gel bonded ODS/SCX particles.

unequal capillary forces generated from the heterogeneous small pores are believed to be responsible for the shrinking and cracking of the dried sol–gel [38]. In the sol–gel bonded column, mechanically strong ODS particles were tightly packed into the column, and the sol–gel matrix shrank and accumulated between the particles, and bonded the particles together. The solvent in the sol–gel matrix was replaced by supercritical CO_2 before drying and the sol–gel was dried by expelling supercritical CO_2. Since the surface tension of a supercritical fluid is zero [38], the capillary forces in the sol–gel matrix were effectively eliminated when the column was dried using supercritical CO_2, leading to a crack-free column bed. Supercritical CO_2 drying also shortened the drying time from days to hours in comparison to conventional thermal drying.

3.2. EOF velocity and standing current

The EOF is generated at the surface of a charged bed under an external electric field. Assuming that there is no electrical double layer overlap, the EOF velocity, μ_{eo}, an be expressed as [14]

$$\nu_{eo} = \mu_{eo}E = \frac{1}{3 \cdot 10^7 |Z| \sqrt{C}} \frac{\sigma}{\eta} E \quad (1)$$

where E, μ_{eo}, σ, η, Z, and C are the applied electric field strength, the electroosmotic mobility, the total excess charge per unit area in the stern plane, the viscosity of the mobile phase, the charges on the buffer ions, and the buffer concentration, respectively. Eq. (1) implies that the EOF velocity depends on the applied electric field strength, and the properties of the mobile and stationary phases.

The current generated in a column can be expressed as [3]:

$$i = E\lambda C\pi\epsilon \frac{d_c^2}{4} \quad (2)$$

where E, λ, C, ϵ, and d_c are the electric field strength, the equivalent conductivity, the molar concentration of the buffer, the porosity of the packed bed and the inner diameter of the capillary column, respectively. Eq. (2) suggests that the current is related to the applied field strength, the conductivity of the buffer ions, the buffer concentration, and the column permeability.

3.3. Applied electric field strength

Fig. 2 shows plots of EOF velocity and current versus applied electric field strength when using 80% acetonitrile aqueous mobile phase containing 1.5 m*M* phosphate buffer at pH 3.0 and thiourea as an EOF marker. The electroosmotic flow increased linearly with an increase in the applied electric field strength as predicted in Eq. (1). The magnitude of the EOF velocity in a 25/34 cm×75 μm I.D. sol–gel bonded 3-μm ODS/SCX continuous-bed column was 1.9 mm s^{-1} at 882 V cm^{-1} applied electric field strength (30 kV), which is comparable to the linear velocity of the mobile phase commonly used in LC. Fig. 2 also shows that the current increased linearly with the applied electric field strength, which suggests that Joule heating in the column can be ignored with an applied electric field strength less than

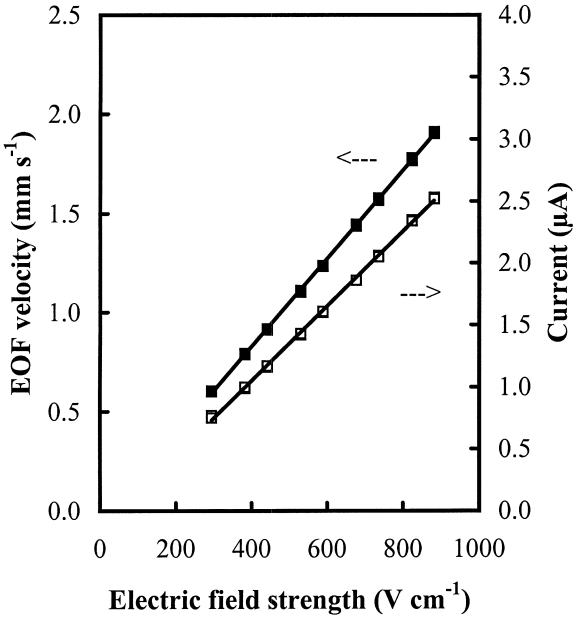

Fig. 2. Plot of EOF velocity (■) and current (□) versus applied electric field strength. Conditions: 25/34 cm×75 μm I.D. continuous-bed column containing sol–gel bonded 3 μm ODS/SCX with 80 Å pores, 80% (v/v) acetonitrile aqueous mobile phase containing 1.5 m*M* phosphate buffer at pH 3.0, 5 kV×2 s electrokinetic injection, 0.3 m*M* thiourea used as EOF marker, 254 nm UV detection.

882 V cm^{-1} (30 kV) under the experimental conditions used in this study.

Just as in sol–gel bonded ODS columns, bubble formation was not observed in 25/34 cm×75 μm I.D. sol–gel bonded ODS/SCX columns with 1.5 m*M* phosphate buffer and up to 882 V cm^{-1} applied electric field strength (30 kV). Bubble formation is often noticed in packed capillary columns, which is believed to result from the end-frits [12]. The absence of bubble formation in the sol–gel bonded columns is possibly due to the easy wettability of the sol–gel bonded columns by the mobile phase and the homogeneity of the column bed. The absence of bubble formation is an advantage over packed columns because it eliminates the requirement for pressurization of the column ends and, thus, simplifies the instrumentation and operation.

3.4. Buffer pH

In our previous study [31], we found that the EOF in a sol–gel bonded ODS column was strongly dependent on the mobile phase pH. The EOF is believed to be due to the dissociation of silanol groups [13]. In this study, we investigated the effect of buffer pH on EOF velocity for sol–gel bonded ODS/SCX columns. Fig. 3 shows plots of EOF velocity and current versus mobile phase pH using 70% acetonitrile aqueous mobile phases with 1.5 m*M* phosphate buffer and an applied electric field strength of 442 V cm^{-1}. As can be seen, the EOF velocity for the sol–gel bonded ODS/SCX column was nearly the same from pH 2–9. The pH independent EOF for the ODS/SCX column implies that the EOF velocity is mainly due to sulfonic acid groups with little contribution from the residual silanol groups. As is well known, sulfonic acid groups have a pK_a less than 2. When the mobile phase pH is greater than 2, the sulfonic acid groups are totally ionized, leading to a stable charge density and, thus, nearly constant EOF velocity as indicated by Eq. (1). The calculated electroosmotic mobility for ODS/SCX columns at pH 2–9 is nearly 2.1 m^2 s^{-1} V^{-1}, which is comparable to that for ODS columns at pH 8, but is two times higher than that for ODS columns at pH less than 5 [31]. The relatively strong EOF for ODS/SCX columns at low pH allows the use of the ODS/SCX columns over a wide pH range. A stable EOF over a wide pH range is also desirable for obtaining reproducible retention times. Fig. 3 also shows that the current generated in the column was related to the mobile phase pH at constant buffer concentration, which is believed to be due to the ionization of phosphate buffer ions. Four anions, hydroxide dihydrogenphosphate, monohydrogenphosphate, and phosphate exist in a phosphate buffer. The distribution coefficients of these anions at buffer pH 2–9 have been calculated from the dissociation constants of phosphoric acid in water, and are readily available. Phosphate and hydroxide ions can be ignored at pH 2–9. Dihydrogenphosphate ions first increase rapidly with an increase in pH from 2 to 4 and then stay nearly constant at pH 4–6, which determines the characteristic current change measured for the mobile phase between pH 2–6 as shown in Fig. 3. Monohydrogenphosphate ions can be ignored at pH less than 6. However, they become the dominant anions as pH increases from 6 to 9, which results in the current change observed in this pH range. Since monohydro-

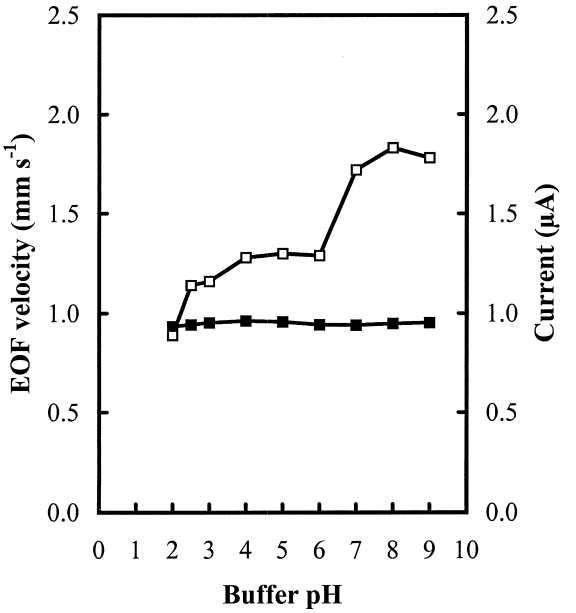

Fig. 3. Plot of EOF velocity (■) and current (□) versus buffer pH. Conditions:70% (v/v) acetonitrile aqueous mobile phase containing 1.5 m*M* phosphate buffer, 442 V cm^{-1} applied electric field strength (15 kV voltage); other conditions are the same as in Fig. 2.

genphosphate has higher conductivity than dihydrogenphosphate, the current at pH 7–9 is higher than that at pH 2–6 as indicated by Eq. (2).

3.5. Buffer concentration

Fig. 4 shows plots of EOF velocity and current versus buffer concentration using 70% acetonitrile aqueous mobile phase with phosphate buffer at pH 3.0 and applied electric field strength of 442 V cm^{-1}. As can be seen, the EOF velocity for the ODS/SCX column decreased slowly as the phosphate buffer concentration increased from 1.0 to 5.0 m*M*, while the current increased nearly linearly with an increase in buffer concentration. The low EOF velocity at high buffer concentration is due to compression of the electrical double layer thickness. A thin electrical double layer leads to a high zeta potential and, thus, a small EOF. The low current at low buffer concentration is due to the low conductivity of the dilute buffer solution as suggested by Eq. (2). Although dilute buffer is good for obtaining high EOF and preventing Joule heating, it can result in fast buffer ion depletion. As a compromise, 1.5 m*M* buffer concentration was used for the separations in this study.

3.6. Acetonitrile content

Fig. 5 shows plots of EOF velocity and current versus acetonitrile content using acetonitrile aqueous mobile phase with a phosphate buffer concentration of 1.5 m*M* at pH 3.0. As can been seen, both EOF velocity and current decreased and then increased with an increase in acetonitrile content in the mobile phase with the lowest EOF velocity and current at 40% acetonitrile aqueous mobile phase. The low EOF velocity at 40% acetonitrile aqueous mobile phase was also reported for sol–gel bonded ODS columns [31] and fused ODS columns [28].

3.7. Column efficiency

Fig. 6 shows plots of plate height versus EOF velocity for unretained solutes using an 80% acetonitrile aqueous mobile phase with 1.5 m*M* phosphate

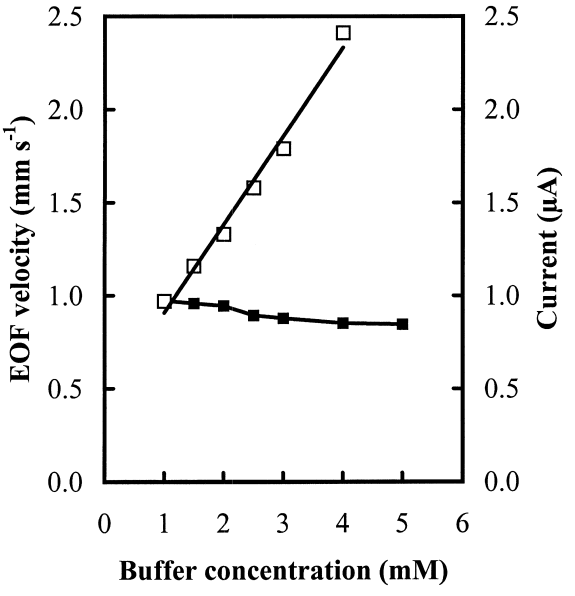

Fig. 4. Plot of EOF velocity (■) and current (□) versus buffer concentration in the mobile phase. Conditions: 70% (v/v) acetonitrile aqueous mobile phase containing phosphate buffer at pH 3.0, 442 V cm^{-1} applied electric field strength (15 kV voltage); other conditions are the same as in Fig. 2.

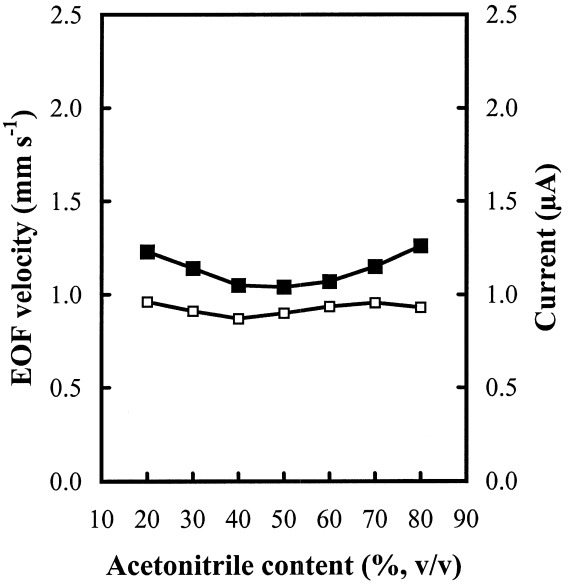

Fig. 5. Plot of EOF velocity (■) and current (□) versus acetonitrile content in the mobile phase. Conditions: acetonitrile aqueous mobile phase containing 1.5 m*M* phosphate buffer at pH 3.0, 442 V cm^{-1} applied electric field strength (15 kV voltage); other conditions are the same as in Fig. 2.

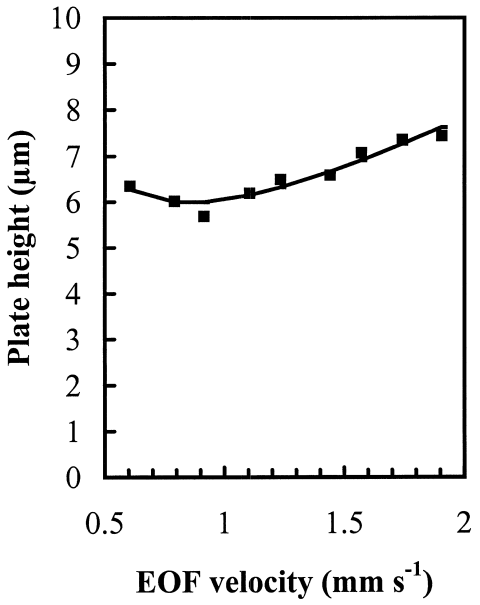

Fig. 6. Plot of plate height versus EOF velocity as measured using thiourea as an unretained solute. Conditions: 25/34 cm×75 μm I.D. continuous-bed column containing sol–gel bonded 3 μm ODS/SCX with 80 Å pores, 80% acetonitrile aqueous mobile phase containing 1.5 m*M* phosphate buffer at pH 3.0, applied electric field strength from 295 to 882 V cm^{-1} (10–30 kV voltage), 5 kV×2 s electrokinetic injection, 0.3 m*M* thiourea used as EOF marker, 254 nm UV detection.

buffer at pH 3.0. The efficiency characteristics of the sol–gel bonded ODS/SCX columns were obtained by fitting the data in Fig. 6 into the van Deemter equation using nonlinear analysis software SISTAT 8.0®. The results are listed in Table 1. A minimum plate height of 5.7 μm (1.75×10^5 plates per meter) for a 34/25 cm×75 μm I.D. column containing sol–gel bonded 3 μm ODS/SCX was obtained at an EOF velocity of 0.92 mm s^{-1}. The efficiency is comparable to a 3 μm ODS packed CEC column. The small A term is believed to result from the plug-like EOF flow.

Table 1
Efficiency characteristics[a] for sol–gel bonded 3 μm ODS/SCX continuous-bed columns[b]

A (μm)	1.20
B ($\times10^3$ μm^2 s^{-1})	2.04
C (10^{-3} s)	2.81
H_{min} (μm)	5.70
N ($\times10^5$ plates m^{-1})	1.75
ν_{opt} (mm s^{-1})	0.92

[a] Measured with unretained thiourea, $k=0$.
[b] Chromatographic conditions are listed in the legend for Fig. 6.

3.8. Separations of aromatic compounds

With typical applied electric field strength, the EOF velocity for ODS columns at pH less than 5.0 is often less than the optimum linear velocity, which results in low efficiency and long separation time. On the other hand, silica-based packing materials can gradually dissolve at pH higher than 8, which can lead to short column lifetime. Therefore, ODS columns can only be used with mobile phases in the limited pH range of 5–8. Furthermore, the EOF velocity for ODS columns change with mobile phase pH [13,31], which can cause irreproducible retention times for real samples. The sol–gel bonded ODS/SCX column had a relatively strong EOF at low pH and a stable EOF over a wide pH range as shown in Fig. 3. Fig. 7 shows a separation of a test mixture of neutral aromatic compounds with different functional groups on a sol–gel bonded ODS/SCX continuous-bed column using an 80% acetonitrile aqueous mobile phase with 1.5 m*M* phosphate buffer at pH 3.0. Six compounds were baseline separated with symmetrical peak shapes in 6 min. The symmetrical peak shape of benzylalcohol in Fig. 7 implies that the sulfonic acid groups on the ODS/SCX particles had no detrimental effect on the separation of such polar compounds under the experimental conditions. Fig. 8 shows a separation of aromatic hydrocarbon homologues on a sol–gel bonded ODS/SCX column using an 80% acetonitrile aqueous mobile phase with 1.5 m*M* phosphate buffer at pH 3.0. The aromatic hydrocarbons eluted according to their carbon numbers

3.9. Retention factors

Table 2 lists the retention factors, *k*, for the test aromatic compounds obtained on a sol–gel bonded ODS/SCX continuous-bed column compared to values obtained using sol–gel ODS continuous-bed columns in our previous study [31]. The data in Table 2 suggest that the ODS/SCX column had stronger retention for polarizable to strongly polar neutral compounds than ODS columns, which is

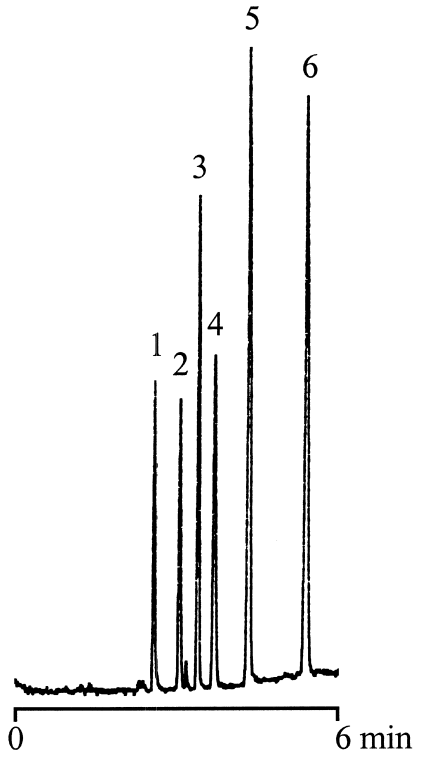

Fig. 7. Electrochromatogram of test neutral aromatic compounds. Conditions: 588 V cm^{-1} applied electric field strength (20 kV voltage); other conditions are the same as in Fig. 6. Peak identifications: (1) thiourea, (2) benzylalcohol, (3) benzaldehyde, (4) dimethylphthalate, (5) benzophenone, and (6) biphenyl.

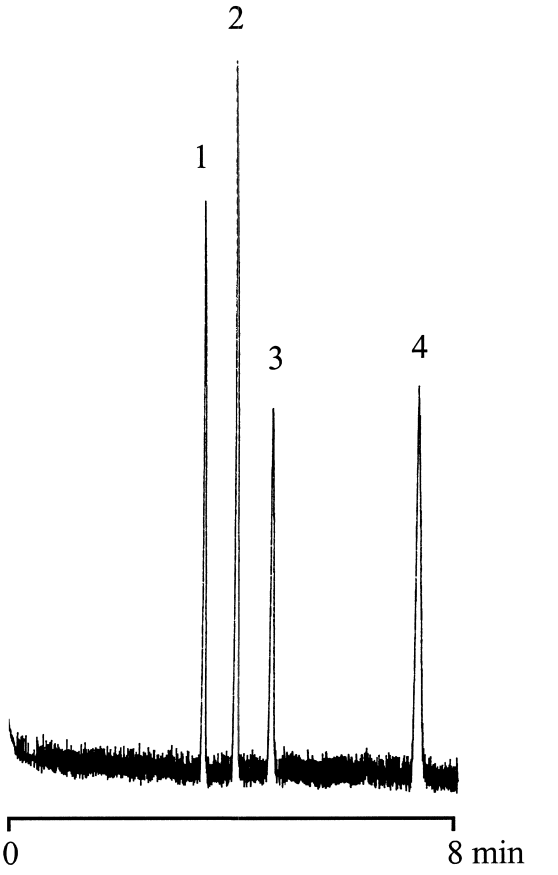

Fig. 8. Electrochromatogram of aromatic hydrocarbon homologues. Conditions: 735 V cm^{-1} applied electric field strength (25 kV voltage); other conditions are the same as in Fig. 6. Peak identifications: (1) benzene, (2) toluene, (3) ethylbenzene, and (4) butylbenzene.

believed to be due to the use of small particle size and/or possibly due to the higher carbon content of the ODS/SCX packing materials. It was observed that the retention of these small neutral compounds increased with a decrease in acetonitrile content, which is typical for reversed-phase separations [31].

3.10. Reproducibility of retention factors

Table 3 lists the run-to-run and column-to-column reproducibilities of retention factors for test aromatic compounds on the sol–gel bonded ODS/SCX column using 80% acetonitrile aqueous mobile phase with 1.5 m*M* phosphate buffer at pH 3.0. Relative standard deviations of retention factors were less than 2.5% for all of the test compounds for 18 runs. Five 25/34 cm×75 μm I.D. sol–gel bonded 3 μm ODS/SCX columns were prepared following the same procedures and using the same batch of packing materials. Relative standard deviations of retention factors were less than 8.0% from column-to-column for all of the test compounds.

4. Conclusions

Continuous-bed columns containing sol–gel bonded silica particles with mixed-mode octadecyl and propylsulfonic acid groups (ODS/SCX) were prepared using a sol–gel procedure. The sol–gel bonded continuous-bed columns demonstrated advantages over packed columns with respect to bubble

Table 2
Retention factors for aromatic compounds on ODS/SCX continuous-bed columns[a]

Compound	Retention factor (k)	
	ODS/SCX (3 μm, 80 Å)	ODS (5 μm, 90 Å) (from Ref. [31])
Benzylalcohol	0.33	0.22
Benzaldehyde	0.75	0.48
Dimethylphthalate	1.38	0.89
Benzophenone	2.44	1.23
Biphenyl	5.14	2.13

[a] Experimental conditions: 60% acetonitrile/aqueous mobile phase. Other conditions are the same as in Fig. 7.

Table 3
Reproducibility of retention factors for aromatic compounds[a]

Compound	Retention factor (k)	
	Mean (RSD) Run-to-run ($n=18$)	Mean (RSD) Column-to-column ($n=5$)
Benzylalcohol	0.18 (2.2)	0.18 (7.5)
Benzaldehyde	0.32 (1.2)	0.33 (6.0)
Dimethylphthalate	0.45 (0.89)	0.44 (3.2)
Benzophenone	0.71 (0.71)	0.70 (3.7)
Biphenyl	1.14 (0.70)	1.14 (2.5)

[a] Experimental conditions are the same as in Fig. 7.

formation. The ODS/SCX columns showed similar retention characteristics as ODS columns. The ODS/SCX columns provided a relatively strong EOF at low pH and a stable EOF throughout pH 2–9, making them useful for separations at low pH and for reproducible separations.

Acknowledgements

The authors thank Professor Peter Myers of Xtec (Stockport, Cheshire, UK) for providing the 3 μm S3 ODS/SCX porous packing materials. This work was funded in part through a collaboration with Sensar Corporation (Provo, UT) under a National Science Foundation Small Business Technology Transfer Program, Grant No. DMI-9705341. Partial support was also provided by G. D. Searle, Research and Development Division, Skokie, IL.

References

[1] V. Pretorius, B.J. Hopkins, J.D. Schieke, J. Chromatogr. 99 (1974) 23.
[2] J.W. Jorgenson, K.D. Lukacs, J. Chromatogr. 218 (1981) 209.
[3] J.H. Knox, I.H. Grant, Chromatographia 24 (1987) 135.
[4] J.H. Knox, Chromatographia 329 (1988) 26.
[5] J.H. Knox, J. Chromatogr. A. 680 (1994) 3.
[6] J.H. Knox, I.H. Grant, Chromatographia 32 (1991) 317.
[7] R.M. Seifar, W.T. Kok, J.C. Kraak, H. Poppe, Chromatographia 46 (1997) 131.
[8] N.W. Smith, M.B. Evans, Chromatographia 41 (1995) 197.
[9] C. Yan, R. Dadoo, H. Zhao, R.N. Zare, D.J. Rakestraw, Anal. Chem. 67 (1995) 2026.
[10] M.M. Dittmann, G.P. Rozing, J. Chromatogr. A 744 (1996) 63.
[11] S.E. van den Bosch, S. Heemstra, J.C. Kraak, H. Hoppe, J. Chromatogr. A 755 (1996) 165.
[12] R.A. Carney, M.M. Robson, K.D. Bartle, P. Myers, J. High Resolut. Chromatogr. 22 (1999) 29.
[13] S. Kitagawa, T. Tsuda, J. Microcol. Sep. 6 (1994) 91.
[14] T. Tsuda, K. Nomura, G. Nakagawa, J. Chromatogr. 248 (1982) 241.
[15] G.J.M. Bruin, P.P.H. Tock, J.C. Kraak, H. Poppe, J. Chromatogr. 517 (1990) 557.
[16] Y. Guo, L.A. Colòn, Anal. Chem. 67 (1995) 2511.
[17] C. Fujimoto, J. Kino, H. Sawada, J. Chromatogr. A 716 (1995) 107.
[18] C. Fujimoto, J.Y. Fujise, E. Matsuzawa, Anal. Chem. 68 (1996) 2753.
[19] C. Ericson, J. Liao, K. Nakazato, S. Hjerten, J. Chromatogr. A 767 (1997) 33.
[20] A. Palm, M.V. Novotny, Anal. Chem. 69 (1997) 4499.

[21] E.C. Peters, M. Petro, F. Svec, J.M. Fréchet, Anal. Chem. 69 (1997) 3646.
[22] E.C. Peters, M. Petro, F. Svec, J.M. Fréchet, Anal. Chem. 70 (1998) 2288.
[23] E.C. Peters, M. Petro, F. Svec, J.M. Fréchet, J. Anal. Chem. 70 (1998) 2296.
[24] J.G. Dorsey, A.S. Lister, P.B. Wright, S.C. Wendelke, T.L. Chester, Presented at the 19th International Symposium on Capillary Chromatography and Electrophoresis, Wintergreen, VA, USA, May, 1997.
[25] A. Malik, J.D. Hayes, D. Wang, S.L. Chong, G.S. Corbett, J.W. Cramer, Presented at the 19th International Symposium on Capillary Chromatography and Electrophoresis, Wintergreen, VA, USA, May, 1997.
[26] N. Isizuka, H. Minakuchi, K. Nakanishi, N. Soga, H. Nagayama, H. Kobayashi, T. Ikegami, K. Hosoya, N. Tanaka, Presented at the 12th International Symposium on High Performance Capillary Electrophoresis and Related Microscale Techniques, Palm Springs, CA, January, 1999.
[27] M.T. Dulay, R.P. Kulkarni, R.N. Zare, Anal. Chem. 70 (1998) 5103.
[28] R. Asiaie, X. Huang, D. Farnan, C. Horvath, J. Chromatogr. A 806 (1998) 251.
[29] T. Adam, K.K. Unger, M.M. Dittmann, G. Rozing, Presented at the 21st International Symposium on High Performance Liquid Phase Separations and Related Techniques. Birmingham, UK, June 1997.
[30] G. Chirica, V.T. Remcho, Electrophoresis 20 (1999) 50.
[31] Q. Tang, B. Xin, M.L. Lee, J. Chromatogr. A 837 (1999) 35.
[32] Q. Tang, N. Wu, M.L. Lee, J. Microcol. Sep. 11 (1999) 550.
[33] M. Zhang, Z. El Rassi, Electrophoresis 19 (1998) 2068.
[34] M. Zhang, Z. El Rassi, Electrophoresis 20 (1999) 31.
[35] N.W. Smith, M.B. Evans, J. Chromatogr. A 832 (1999) 41.
[36] M.M. Dittmann, G.P. Rozing, J. Microcol. Sep. 9 (1997) 399.
[37] A. Malik, W. Li, M.L. Lee, J. Microcol. Sep. 5 (1993) 361.
[38] C.J. Brinker, G.W. Scherer, Sol–gel Science: The Physics and Chemistry of Sol–gel Processing, Academic Press, San Diego, CA, USA, 1990.